LA-UR-18-29007
Approved for public release; distribution is unlimited.

Title: A Low Order Mimetic Finite Difference Method for Resistive Magnetohydrodynamics in 2D

Author(s): Naranjo, Sebastian
Gyrya, Vitaliy

Intended for: Report

Issued: 2018-09-21

A Low Order Mimetic Finite Difference Method for Resistive Magnetohydrodynamics in 2D

Sebastian Naranjo and Vitaliy Gyrya

September 12, 2018

Abstract

We developed a low order Mimetic Finite Difference (MFD) discretization for the equations of magnetohydrodynamics (MHD) in two space dimensions. These equations describe the evolution of the electric and magnetic fields in the presence of prescribed velocity field. The method is designed to work on general polygonal meshes and preserves the divergence-free condition on the magnetic field. The electric field is discretized at the vertices/nodes and the magnetic field uses edge-based discretization. The method reconstructs the magnetic field to extract nodal values necessary to approximate some terms present in Ohm's law. We test the robustness of our numerical scheme on three different types of meshes: with triangular elements, quadrilateral and unstructured polyhedrons obtain from a Voronoi tesselation. Analysis of the convergence for each of the aforementioned mesh types is presented. We finish with a test problem that shows the method is capable of modelling magnetic reconnection.

Contents

1 Introduction

Interest in the behavior of plasmas has skyrocketed in the modern age with applications ranging from fusion-based nuclear power to low power thrusters for contemporary spacecraft. Since the late 1930s or beginning of 1940s, efforts have been devoted to models that are faithful to its dynamics, an approach that has proven successful and has become standard is to consider plasmas as magnetized fluids, an area called magnetohydrodynamics or MHD for short. Therefore, the description of these plasmas follow from a blending together of electromagnetic theory and fluid flow. Research in MHD is driven at a minimum by four communities: Astrophysicists that study accretion discs and the dynamics that rule stars, planetary scientists that are interested in the generation of magnetic fields by the core of planets, plasma physicists whose interest lies in the confinement of plasmas by means of external magnetic fields and engineers which have found that with external magnetic fields they can control the motion of liquid metals leading to a revolution in metallugical techniques in industry.

There are different types of models in MHD differing by the version of Ohm's law employed. The simplest is that of ideal MHD, the main assumption being that the fluid is considered to be a perfect conductor, here Ohm's law is

$$\vec{E} + \vec{u} \times \vec{B} = 0,$$

where $\vec{E}$, $\vec{u}$ and $\vec{B}$ represent the electric field, fluid flow velocity and magnetic field respectively. Although ideal MHD has proven to be accurate in many applicacions, Lenz's law dictates that the magnetic field lines must move with the fluid even as it is twisted or distorted, a result called Alfvén's theorem, and is therefore incapable of describing important features of the behaviour of plasmas like magnetic reconnection, a phenomenon in which the magnetic field line change topology. An alternative is referred to as resistive MHD and differs in that version fo Ohm's law employed is

$$\vec{E} + \vec{u} \times \vec{B} = \nu \vec{J}.$$

Introducing $\vec{J}$ as the current density and ν as the resistivity. However, if the magnetic reconnection is fast then resistive MHD proves insufficient in its description.

In the absence of a magnetic field electrical currents, in a conductor, flow in a straight line. However, if a magnetic field with a non-negligible component perpendicular to the flow of the charges is present then these particles experience a force, the Lorentz force, that curves the path these particles follow leading to an accumulation of charge in the sides of the conductive material. The outcome being a voltage that runs accross the conductor and an uneven distribution of charge. This phenomenon is referred to as the Hall effect and including this effect in our MHD model leads to a robust description of the behaviour of a plasma that is effective in describing even complicated phenomena like fast magnetic reconnection. From a mathematical perspective

the difference lies in adding a new term, a non-linear term, to Ohm's law leading to the system

$$\text{Faraday's Law} \qquad \frac{\partial}{\partial t}\vec{B} = -\nabla \times \vec{E}, \tag{1a}$$

$$\text{Ohm's Law With Hall Effect} \qquad \vec{E} = -\vec{u} \times \vec{B} + \nu\vec{J} + C\vec{J} \times \vec{B}, \tag{1b}$$

$$\text{Ampere's Law} \qquad \vec{J} = \nabla \times \vec{B}, \tag{1c}$$

A model termed as Hall MHD which we will take as valid in bounded volume D with smooth boundary. It is important to note that (1) is not a complete system if the velocity is unknown, a larger system including equations arising from conservation principles would complete the system. However, in this report we will consider that the flow is controlled and therefore $\vec{u}$ is a known quantity. A detailed overview of MHD is the one presented in [3].

Hall MHD is notorious for its complicated structure and very little theoretical analysis has been developed, a more fruitful approach is develop numerical techniques to approximate solutions, see for example the finite difference methods developed in [1]. Hence, the aim of this report is to develop a numerical scheme to compute approximations of the electric and magnetic fields as they are described in (1) using the Mimetic Finite Difference (MFD) method. Differential geometry and PDE theory based on functional analysis provide a powerful set of tools to analyse systems like that of (1). It is the guiding philosophy of MFD to construct, on a sequence of meshes, a discrete version of tensor calculus from where a discrete mimicry of the techniques in differential geometry and PDE theory can be formulated. The advantages of the MFD framework lie in the generality of the meshes it admits, a topic that will be discussed in section 3, and in the fact that the framework gives rise to a family of schemes from where some schemes may be optimal for different modelling purposes: dispersion relations, maximum principles, a process called M-adaptation. A recommended source for theory on the MFD method is [2] and for the process of M-adaptation [5].

The report is organized as follows: we begin by downscaling (1) to a problem in two dimensions then we postulate the mimetic formulation which which is proceeded by the definition of degrees of freedom and the mimetic matrices that appear in the formulation, the report ends with an exposition of the numerical experimentation.

2 Problem formulation

Although the ultimate goal is to solve the system (1), in order to avoid much of the computational complexity, as a first step, we will reduce this problem to one in two dimensions this is the main goal of the present section.

Let us begin by breaking up the different vector quantities in (1) into their components on the plane and those in the $z-$direction. In what remains of this report we shall denote them as follows

$$\vec{u} = \begin{pmatrix} \mathbf{u} \\ u_z \end{pmatrix}, \quad \vec{E} = \begin{pmatrix} \mathbf{E} \\ E_z \end{pmatrix}, \quad \vec{J} = \begin{pmatrix} \mathbf{J} \\ J_z \end{pmatrix} \text{ and } \vec{B} = \begin{pmatrix} \mathbf{B} \\ B_z \end{pmatrix}.$$

Moreover let **curl** represent the $1-$D to $2-$D rotational operator, curl the $2-$D to $1-$D rotational and e_1, e_2 the canonical basis in $\mathbb{R}^2$. Using this notation we can decompose the

operators in (1) into

$$\begin{aligned}
\nabla \times \vec{E} &= \begin{pmatrix} \mathbf{curl} E_z - \frac{\partial}{\partial z} E_y e_1 + \frac{\partial}{\partial z} E_x e_2 \\ \mathrm{curl}\mathbf{E} \end{pmatrix} & \nabla \times \vec{B} &= \begin{pmatrix} \mathbf{curl} B_z - \frac{\partial}{\partial z} B_y e_1 + \frac{\partial}{\partial z} B_x e_2 \\ \mathrm{curl}\mathbf{B} \end{pmatrix} \\
\vec{u} \times \vec{B} &= \begin{pmatrix} \mathbf{u} \times B_z + u_z \times \mathbf{B} \\ \mathbf{u} \times \mathbf{B} \end{pmatrix} & \vec{J} \times \vec{B} &= \begin{pmatrix} \mathbf{J} \times B_z + J_z \times \mathbf{B} \\ \mathbf{J} \times \mathbf{B} \end{pmatrix}.
\end{aligned} \tag{2}$$

We proceed to assume that the evolution of the electric and magnetic fields, on the plane, depends exclusively on the variables proper to the plane rather than what may occur in the $z-$direction. This is to say that

$$\frac{\partial}{\partial z}\mathbf{B} = \vec{0} \text{ and } \frac{\partial}{\partial z}\mathbf{E} = \vec{0}, \tag{3}$$

This assumption, together with the identities in (2), allows us to express the three dimensional rotational in terms of the lower dimensional rotational operators as

$$\nabla \times \vec{E} = \begin{pmatrix} \mathbf{curl} E_z \\ \mathrm{curl}\mathbf{E} \end{pmatrix} \text{ and } \nabla \times \vec{B} = \begin{pmatrix} \mathbf{curl} B_z \\ \mathrm{curl}\mathbf{B} \end{pmatrix},$$

leading us to the decoupling of (1) featured below

$$\begin{cases} \frac{\partial}{\partial t}\mathbf{B} = -\mathbf{curl} E_z \\ \frac{\partial}{\partial t} B_z = -\mathrm{curl}\mathbf{E} \end{cases} \tag{4a}$$

$$\begin{cases} \mathbf{E} = -(\mathbf{u} \times B_z + u_z \times \mathbf{B}) + \nu \mathbf{J} + C(\mathbf{J} \times B_z + \nu J_z \times \mathbf{B}) \\ E_z = -\mathbf{u} \times \mathbf{B} + \nu J_z + C\mathbf{J} \times \mathbf{B} \end{cases} \tag{4b}$$

$$\begin{cases} \mathbf{J} = \mathbf{curl} B_z \\ J_z = \mathrm{curl}\mathbf{B} \end{cases} \tag{4c}$$

We will further assume that the motion of the gas and the evolution of the magnetic field in the $z-$direction are controlled, this is to say that $\vec{u}$ and B_z are known. Therefore, the problem that we will be considering is as follows.

$$\begin{aligned}
&\text{Find } \mathbf{B}, E_z, J_z \text{ such that:} \\
&\qquad \frac{\partial}{\partial t}\mathbf{B} = -\mathbf{curl} E_z \\
&\qquad E_z = -\mathbf{u} \times \mathbf{B} + \nu J_z + C\mathbf{J} \times \mathbf{B} \\
&\qquad J_z = \mathrm{curl}\mathbf{B},
\end{aligned} \tag{5}$$

where $\mathbf{J} = \mathbf{curl} B_z$ and $\mathbf{u}$ are known. This system can, equivalently, be written as bellow.

$$\text{Find } \mathbf{B}, E_z \text{ such that:} \tag{6a}$$

$$\frac{\partial}{\partial t}\mathbf{B} = -\mathbf{curl} E_z \tag{6b}$$

$$E_z = -\mathbf{u} \times \mathbf{B} + \nu \mathrm{curl}\mathbf{B} + C\mathbf{J} \times \mathbf{B}. \tag{6c}$$

It is important to recall that, from electromagnetic theory, magnetic fields must be solenoidal. This condition and assumption (3) imply that

$$\frac{\partial^2}{\partial z^2} B_z = \mathrm{div}_2 \frac{\partial}{\partial z}\mathbf{B} + \frac{\partial^2}{\partial z^2} B_z = \frac{\partial}{\partial z}\mathrm{div}_3 \vec{B} = 0,$$

an immediately consequence is that $B_z = a(x,y)z + b(x,y)$. If we strengthen this condition so that $\partial_z B_z = 0$ then

$$\mathrm{div}_3 \vec{B} = \mathrm{div}_2 \mathbf{B}.$$

Hence if we guarantee that $\mathbf{B}$ at $t = 0$ is solenoidal then from equation (6b) we have that

$$0 = \mathrm{div}_2 \left(\frac{\partial \mathbf{B}}{\partial t} + \mathbf{curl} E_z \right) = \frac{\partial}{\partial t}\mathrm{div}_2 \mathbf{B},$$

in which case the the three dimensional divergence free condtion will remain true for all $t > 0$. This is a property we will incorporate into our mimetic scheme.

3 The Mimetic Finite Difference Formulation

This section is dedicated to finding a discrete formulation for equation (6). We will present the mimetic approximation to the continuous operators in the differential system while their precise definition will be left for later sections.

Let Ω be the projection, onto the plane, of the three dimensional domain D introduced for (1) and further assume that Ω is polygonal. And let us complete the system (6) by adding initial and boundary conditions

$$\text{Find} \quad \mathbf{B}, E \quad \text{such that} \tag{7a}$$

$$\frac{\partial}{\partial t}\mathbf{B} = -\mathbf{curl} E \qquad \text{in} \quad \Omega, \tag{7b}$$

$$E = -\mathbf{u} \times \mathbf{B} + \nu \mathrm{curl} \mathbf{B} + C\mathbf{J} \times \mathbf{B} \qquad \text{in} \quad \Omega, \tag{7c}$$

$$\mathbf{B}(x,y,0) = \mathbf{B}_0(x,y) \qquad \text{in} \quad \Omega, \tag{7d}$$

$$E(x,y,t) = E_0(x,y,t) \qquad \text{in} \quad \partial\Omega. \tag{7e}$$

Since, from this point forward, every problem posed will be in $\mathbb{R}^d$, $d = 1,2$ then the subscript z is unnecessary and will only make the notation heavier hence our choice to drop it. We will distinguish quantities in $\mathbb{R}^2$ with bold outlines while scalar quantities will not be bold.

Let us introduce the spaces that will serve as setting for the rest of the report.

$$H(\mathbf{curl}, \Omega) := \left\{ E : \Omega \to \mathbb{R} : E \in L^2(\Omega), \mathbf{curl} E \in \left(L^2(\Omega) \right)^2 \right\}, \tag{8a}$$

$$\mathbf{H}\left(\mathrm{div}, \Omega\right) := \left\{ \mathbf{B} : \Omega \to \mathbb{R}^2 : \mathbf{B} \in \left(L^2(\Omega) \right)^2, \mathrm{div} \mathbf{B} \in L^2(\Omega) \right\} \tag{8b}$$

, Moreover, we define $H_0(\mathbf{curl}, \Omega)$ as those functions in $H(\mathbf{curl}, \Omega)$ that vanish on the boundary of Ω. After the change of variables $E = E_{\mathsf{Int}} + E_0$ the variational formulation of (7) reads:

find $\mathbf{B} \in C^1([0,\infty), \left(L^2(\Omega)\right)^2)$ *and* $E_{\mathsf{Int}} \in C([0,\infty), H_0(\mathbf{curl}, \Omega))$ *such that*

$$\int_\Omega \frac{\partial \mathbf{B}}{\partial t} \cdot \widetilde{\mathbf{B}} + \int_\Omega \mathbf{curl} E \cdot \widetilde{\mathbf{B}} = 0 \qquad \forall \widetilde{\mathbf{B}} \in \left(L^2(\Omega)\right)^2 \tag{9a}$$

$$\int_\Omega \nu^{-1} E_{\mathsf{Int}} \tilde{E} - \int_\Omega \mathbf{B}\mathbf{curl}\tilde{E} - \int_\Omega \nu^{-1} (C\mathbf{J} - \mathbf{u}) \times \mathbf{B}\tilde{E} = -\int_\Omega \nu^{-1} E_0 \tilde{E} \qquad \forall \tilde{E} \in H_0(\mathbf{curl}, \Omega) \tag{9b}$$

$$\mathbf{B}(x, y, 0) = \mathbf{B}_0(x, y) \qquad \text{in} \quad \Omega, \tag{9c}$$

where we assume that the resistivity, ν, is strongly elliptic, i.e. that there exists $\kappa_1, \kappa_2 > 0$ such that

$$\kappa_1 \leq \nu(x, y) \leq \kappa_2 \qquad \text{almost everywhere in } \Omega.$$

Let, for $h \in (0, \mathrm{Diam}\Omega)$, Ω_h represent a mesh of Ω with mesh size h that satisfies the regularity conditions presented in [4] which, for the sake of completion, we list below

HG *Star-shape regularity*: there exists a positive integer N_s and a positive real number $\rho_s > 0$ such that every mesh Ω_h admits a sub-partition S^h into shape-regular tetrahedra such that:

HG1 every Polyhedron E in Ω_h has a Lipschitz boundary and admits a decomposition made of less than N_s tetrahedra.

HG2 the shape regularity of the tetrahedra E of S^h is defined as follows: the ratio between the radius r_T of the largest inscribed ball and the diameter h_T of the tetrahedron T is bounded from below by $\rho_s > 0$.

HG3 There exist a positive number $\tau*$ such that each element is star shaped with respect to all points in a ball of radius $\tau * h_E$ centered at an internal point of E.

In the Mimetic Method, we define discrete analogs of $\mathbf{B}$ and E which we will denote $\mathbf{B}_h$ and E_h respectively and assume that they belong to vector spaces $\mathscr{E}_h$ and $\mathscr{V}_h$. Let $V_{h,0}$ be the analog of functions in $H_0(\mathbf{curl}, \Omega)$, with these definitions we can pose a discrete mimicry of the variational formulation (9) which we present below and

Find $\mathbf{B}_h \in C^1([0,\infty), \mathscr{E}_h)$ and $E_{h,\mathsf{Int}} \in C([0,\infty), \mathscr{V}_{h,0})$ such that:

$$\left[\widetilde{\mathbf{B}}_h, \frac{\partial}{\partial t}\mathbf{B}_h\right]_{\mathscr{E}_h} + \left[\widetilde{\mathbf{B}}_h, \mathrm{curl}_h(E_{h,\mathsf{Int}} + E_{h,\mathsf{Bound}})\right]_{\mathscr{E}_h} = 0 \qquad \forall \widetilde{\mathbf{B}}_h \in \mathscr{E}_h, \tag{10a}$$

$$\left[\tilde{E}_h, E_{h,\mathsf{Int}}\right]_{\mathscr{V}_h} - \left[\mathrm{curl}_h \tilde{E}_h, \mathbf{B}_h\right]_{\mathscr{E}_h} - \left[\tilde{E}_h, \mathbf{B}_h\right]_{\mathbf{u},\mathbf{J}} = -\left[\tilde{E}_h, E_{h,\mathsf{Bound}}\right]_{\mathscr{V}_h} \qquad \forall \tilde{E}_h \in \mathscr{V}_{h,0}, \tag{10b}$$

$$\mathbf{B}_h(0) = \mathscr{I}_h^{\mathscr{E}}(\mathbf{B}_0). \tag{10c}$$

Here the approximation of the electric field is given by $E_h = E_{h,\mathsf{Int}} + E_{h,\mathsf{Bound}}$, $\mathscr{I}_h^{\mathscr{E}}$ takes functions in $\mathbf{H}(\mathrm{div}, \Omega)$ and returns their discrete representation in $\mathscr{E}_h$ and $\mathrm{curl}_h : \mathscr{V}_h \to \mathscr{E}_h$ is a discrete analog of the continuous vector rotational. Moreover, the discrete bilinear forms presented are approximations of the quantities featured

$$[\tilde{E}_h, E_h]_{\mathscr{V}_h} \approx \int_\Omega \nu^{-1} \tilde{E} E, \qquad [\widetilde{\mathbf{B}}_h, \mathbf{B}_h]_{\mathscr{E}_h} \approx \int_\Omega \widetilde{\mathbf{B}} \cdot \mathbf{B}, \qquad [E_h, \mathbf{B}_h]_{\mathbf{u},\mathbf{J}} \approx \int_\Omega \nu^{-1} E(\mathbf{u} - C\mathbf{J}) \times \mathbf{B}. \tag{11}$$

4 Definition Of Degrees Of Freedom And Primary Operators

In this section we define the discrete representation of functions in $H(\mathbf{curl},\Omega)$, $\mathbf{H}\big(\mathrm{div},\Omega\big)$ and the operators that act on these spaces, namely the rotational and divergence.

As before let, for $h \in (0, \mathrm{Diam}\Omega)$, the set Ω_h represent a mesh of Ω with mesh-size h satisfying the HG, HG1-HG3 conditions in the previous section. Moreover define $\mathcal{V}$, $\mathcal{E}$, $\mathcal{F}$ be the sets of vertices, edges and elements in Ω_h. For functions in $H(\mathbf{curl},\Omega)$ that are sufficiently regular we define their interpolation, $\mathcal{I}_h^{\mathcal{V}}$, by

$$\mathcal{I}_h^{\mathcal{V}}(E) := (E_v)_{v\in\mathcal{V}}, \quad E_v = E(v).$$

Likewise, the interpolation of functions in $\mathbf{H}\big(\mathrm{div},\Omega\big)$ and $L^2(\Omega)$ will be

$$\mathcal{I}_h^{\mathcal{E}}(\mathbf{B}) := (B_e)_{e\in\mathcal{E}}, \quad B_e = \frac{1}{|e|}\int_e B\cdot\hat{n}d\ell, \qquad \mathcal{I}_h^{\mathcal{F}}(p) := \big(p_f\big)_{f\in\mathcal{F}}, \quad p_f = \frac{1}{|P|}\int_P p dA, \tag{12}$$

respectively, where $\hat{n}$ is a unit-vector normal to the edge $e = (v_1, v_2)$ that we will pick as by rotating the unit tangent, on e, in the counterclockwise direction.

The image of $\mathcal{I}_h^{\mathcal{F}}$, $\mathcal{I}_h^{\mathcal{E}}$ and $\mathcal{I}_h^{\mathcal{F}}$ will be denoted $\mathcal{V}_h$, $\mathcal{E}_h$ and $\mathcal{F}_h$ and referred to as the set of vertex-based function edge-based and element-based functions respectively.

Let us proceed to define the primary opertaors. The primary curl operator, denoted $\mathrm{curl}_h : \mathcal{V}_h \to \mathcal{E}_h$, evaluated on an edge e with endpoints v_1 and v_2 is

$$\big(\mathrm{curl}_h E_h\big)_{e=(v_1,v_2)} = \left(\frac{E_{v_2} - E_{v_1}}{|e|}\right). \tag{13}$$

A moment's reflection on the relation between the unit tangent, $\hat{\tau}$, along an edge, e and $\hat{n}$ will reveal that

$$\nabla E\cdot\hat{\tau} = \mathbf{curl}E\cdot\hat{n} \tag{14}$$

Assuming that $\hat{n}$ is obtained by rotating $\hat{\tau}$ in the counterclockwise direction, furthermore notice that, for $e = (v_1, v_2)$, from (14) and the fundamental theorem of line integrals we can deduce that

$$\begin{aligned}\Big(\mathrm{curl}_h\circ\mathcal{I}_h^{\mathcal{V}}(E)\Big)_{e=(v_1,v_2)} &= \frac{E(v_2)-E(v_1)}{|e|} = \\ &= \frac{1}{|e|}\int_e \nabla E\cdot\hat{\tau}d\ell = \frac{1}{|e|}\int_e \mathbf{curl}E\cdot\hat{n}d\ell = \Big(\mathcal{I}_h^{\mathcal{E}}\circ\mathbf{curl}(E)\Big)_e.\end{aligned} \tag{15}$$

Tha above statement shows that the codomain of curl_h is $\mathcal{E}_h$, as previously stated. Let us now define the discrete divergence, we can do this by a mimicry of the divergence theorem on a cell $P = (e_1, ...e_N)$, note that

$$\int_P \mathrm{div}\mathbf{B}dA = \sum_{i=1}^N \beta_{e_i}\int_{e_i}\mathbf{B}\cdot\hat{n}d\ell = \sum_{i=1}^N |e_i|\beta_{e_i}\mathcal{I}_h^{\mathcal{E}}(\mathbf{B})_{e_i}, \tag{16}$$

where $\beta_e \in \{-1, 1\}$ is picked in order to guarantee that the vector $\beta_e \hat{n}$ has the direction required by the divergence theorem. Inspired by (16) we define the discrete divergence, $\mathrm{div}_h : \mathscr{E}_h \to \mathscr{F}_h$, by

$$\left(\mathrm{div}_h \mathbf{B}_h\right)_{P=(e_1,\ldots,e_N)} = \frac{1}{|P|} \sum_{i=1}^{N} |e_i| \beta_{e_i} \left(\mathbf{B}_h\right)_{e_i}. \tag{17}$$

Hence, from the definition of degrees of freedom in $\mathscr{F}_h$ presented in (12) and equations (16) and (17) we find that

$$\left(\mathrm{div}_h \circ \mathscr{I}_h^{\mathscr{E}}(\mathbf{B})\right)_P = \frac{1}{|P|} \int_P \mathrm{div}\mathbf{B} dA = \left(\mathscr{I}_h^{\mathscr{F}} \circ \mathrm{div}(\mathbf{B})\right)_P, \tag{18}$$

which, again, ensures that the codomain of this opertator is the one previously stated. These results can be summarized in the following theorem.

Theorem 4.1. *The diagram*

$$\begin{array}{ccccc} H(\boldsymbol{curl}, \Omega) & \xrightarrow{\boldsymbol{curl}} & \mathbf{H}\left(div, \Omega\right) & \xrightarrow{div} & L^2(\Omega) \\ \downarrow \mathscr{I}_h^{\mathscr{V}} & & \downarrow \mathscr{I}_h^{\mathscr{E}} & & \downarrow \mathscr{I}_h^{\mathscr{F}} \\ \mathscr{V}_h & \xrightarrow{curl_h} & \mathscr{E}_h & \xrightarrow{div_h} & \mathscr{F}_h \end{array}$$

is commutative and the chain

$$\{0\} \xrightarrow{0} \mathscr{V}_h \xrightarrow{curl_h} \mathscr{E}_h \xrightarrow{div_h} \mathscr{F}_h \xrightarrow{0} \{0\}$$

is short and exact.

Proof. The commuativity of the diagram above follows from equations (15) and (18). Notice that for $E_h \in \mathscr{E}_h$ and element $P = (e_1, \ldots, e_N)$ where $e_i = (v_i, v_{i+1})$ then

$$\mathrm{div}_h \circ \mathrm{curl}_h E_h = \frac{1}{|P|} \sum_{i=1}^{N} (E_h)_{v_{i+1}} - (E_h)_{v_i} = (E_h)_{v_{N+1}} - (E_h)_{v_1},$$

but since the boundary of P is a closed loop we must have that $v_{N+1} = v_1$ and so

$$\mathrm{div}_h \circ \mathrm{curl}_h E_h = 0.$$

To finish the proof of exactness of the short chain presented in the statement of the theorem suppose that $\mathbf{B}_h \in \mathscr{E}_h$ is such that $\mathrm{div}_h \mathbf{B}_h \equiv \vec{0}$ then if we select E to be such that when restricted to an element P it solves

$$-\triangle p = 0 \text{ in } P$$
$$\alpha_e \nabla p \cdot \hat{n} = (\mathbf{B}_h)_e \text{ on } e \text{ forall e in the boundary of } P.$$

Since $\mathrm{div}\nabla p = 0$ then there must exist $E \in H(\mathbf{curl}, \Omega)$ such that $\nabla p = \mathbf{curl} E$ defining $\mathbf{B} = \mathbf{curl} E$ we find that for any edge

$$\left(\mathscr{I}_h^{\mathscr{E}}(\mathbf{B})\right)_e = \frac{1}{|e|} \int_e \mathbf{curl} E \cdot \hat{n} d\ell = \frac{\alpha_e}{|e|} \int_e \nabla p \cdot \hat{\tau} d\ell = (\mathbf{B}_h)_e,$$

and by the commuting property

$$\mathbf{B}_h = \mathscr{I}_h^{\mathscr{E}}(\mathbf{B}) = \mathrm{curl}_h \left(\mathscr{I}_h^{\mathscr{V}}(E)\right).$$

This completes the proof. □

5 Discretization

In this section we present the algorithm derived from the mimetic method. We begin with the mimicry of the variational fomulation presented in the set of equations (10) which, for the convenience of the reader, we rewrite below

Find $\mathbf{B}_h \in C^1([0,\infty), \mathscr{E}_h)$ and $E_{h,\mathsf{Int}} \in C([0,\infty), \mathscr{V}_{h,0})$ such that:

$$\left[\widetilde{\mathbf{B}}_h, \frac{\partial}{\partial t}\mathbf{B}_h\right]_{\mathscr{E}_h} + \left[\widetilde{\mathbf{B}}_h, \mathsf{curl}_h(E_{h,\mathsf{Int}} + E_{h,\mathsf{Bound}})\right]_{\mathscr{E}_h} = 0 \qquad \forall \widetilde{\mathbf{B}}_h \in \mathscr{E}_h, \tag{19a}$$

$$\left[\tilde{E}_h, E_{h,\mathsf{Int}}\right]_{\mathscr{V}_h} - \left[\mathsf{curl}_h \tilde{E}_h, \mathbf{B}_h\right]_{\mathscr{E}_h} - \left[\tilde{E}_h, \mathbf{B}_h\right]_{\mathbf{u},\mathbf{J}} = -\left[\tilde{E}_h, E_{h,\mathsf{Bound}}\right]_{\mathscr{V}_h} \qquad \forall \tilde{E}_h \in \mathscr{V}_{h,0}, \tag{19b}$$

$$\mathbf{B}_h(0) = \mathscr{I}_h^{\mathscr{E}}(\mathbf{B}_0). \tag{19c}$$

Each of the bilinear forms in the expressions above will be represented using a matrix, whose constructions is topic for the proceeding sections. Let us introduce these matrices

$$\left[\widetilde{\mathbf{B}}_h, \mathbf{B}_h\right]_{\mathscr{E}_h} = \widetilde{\mathbf{B}}_h^T \mathbb{M}_{\mathscr{E}} \mathbf{B}_h, \qquad \left[\tilde{E}_h, E_h\right]_{\mathscr{V}_h} = \tilde{E}_h^T \mathbb{M}_{\mathscr{V}} E_h \quad \text{and} \quad \left[\tilde{E}_h, \mathbf{B}_h\right]_{\mathbf{u},\mathbf{J}} = \tilde{E}_h^T \mathbb{M}_{\mathbf{u},\mathbf{J}} \mathbf{B}_h.$$

The matrices, $\mathbb{M}_{\mathscr{V}}$ and $\mathbb{M}_{\mathscr{E}}$ are symmetric and positive definite while the symmetry and definitiveness of $\mathbb{M}_{\mathbf{u},\mathbf{J}}$ will depend on the term $\mathbf{u} - C\mathbf{J}$. With these definitions we can write (19a) as

$$\widetilde{\mathbf{B}}_h^T \mathbb{M}_{\mathscr{E}} \frac{\partial}{\partial t} = -\widetilde{\mathbf{B}}_h^T \mathbb{M}_{\mathscr{E}} \mathsf{curl}_h(E_{h,\mathsf{Int}} + E_{h,\mathsf{Bound}}) \qquad \forall \widetilde{\mathbf{B}}_h \in \mathscr{E}_h,$$

which immediately implies that

$$\frac{\partial}{\partial t}\mathbf{B}_h = -\mathsf{curl}_h(E_{h,\mathsf{Int}} + E_{h,\mathsf{Bound}}). \tag{20}$$

To find a discretization for (19b) that we can implement we introduce the diagonal matrix D defined such that $D_{i,i} = 1$ if and only if the i-th node in our ennumeration is not on the boundary of Ω_h, let $D_{i,i} = 0$ otherwise. The importance of D lies in the fact that left multiplication by this matrix takes an element of $\mathscr{V}_h$ to $\mathscr{V}_{h,0}$. Making use of the matrix D we can write (19b) as

$$\tilde{E}_h^T D \mathbb{M}_{\mathscr{V}} E_{h,\mathsf{Int}} - \tilde{E}_h^T D \mathsf{curl}_h^T \mathbb{M}_{\mathscr{E}} \mathbf{B}_h - D\mathbb{M}_{\mathbf{u},\mathbf{J}} \mathbf{B}_h = -\tilde{E}_h^T D \mathbb{M}_{\mathscr{V}} E_{h,\mathsf{Bound}} \qquad \forall \tilde{E}_h \in \mathscr{V}_h,$$

or equivalently

$$D\mathbb{M}_{\mathscr{V}} E_{h,\mathsf{Int}} - D\mathsf{curl}_h^T \mathbb{M}_{\mathscr{E}} \mathbf{B}_h - D\mathbb{M}_{\mathbf{u},\mathbf{J}} \mathbf{B}_h = -D\mathbb{M}_{\mathscr{V}} E_{h,\mathsf{Bound}}, \tag{21}$$

where, E_{Int} is zero on every entry related to the boundary nodes and $E_{h,\mathsf{Bound}}$ is zero on every interior node. Recalling that $E_h = E_{h,\mathsf{Int}} + E_{h,\mathsf{Bound}}$ and keeping in mind that not all entries of E_h are unknown we can write (20), (21) and (19c) as

$$\frac{\partial}{\partial t}\mathbf{B}_h = -\mathsf{curl}_h E_h \tag{22a}$$

$$D\mathbb{M}_{\mathscr{V}} E_h = D\left(\mathsf{curl}_h^T \mathbb{M}_{\mathscr{E}} + \mathbb{M}_{\mathbf{u},\mathbf{J}}\right)\mathbf{B}_h \tag{22b}$$

$$\mathbf{B}_h(0) = \mathscr{I}_h^{\mathscr{E}}(\mathbf{B}_0). \tag{22c}$$

Now we discretize the time variable on a staggered grid. Equations (22) become

$$\mathbf{B}_h^{n+1} = \mathbf{B}_h^n - \Delta t \mathrm{curl}_h E_h^{n+1/2} \tag{23a}$$

$$D\mathbb{M}_{\mathcal{V}} E_h^{n+1/2} = D\left(\mathrm{curl}_h^T \mathbb{M}_{\mathcal{E}} + \mathbb{M}_{\mathbf{u},\mathbf{J}}\right) \frac{\mathbf{B}_h^{n+1} + \mathbf{B}_h^n}{2}. \tag{23b}$$

Plugging (23a) into (23b) we arrive at

$$D\left(\mathbb{M}_{\mathcal{V}} + \frac{\Delta t}{2}\left(\mathrm{curl}_h^T \mathbb{M}_{\mathcal{E}} + \mathbb{M}_{\mathbf{u},\mathbf{J}}\right)\mathrm{curl}_h\right) E_h^{n+1/2} = D\left(\mathrm{curl}_h^T \mathbb{M}_{\mathcal{E}} + \mathbb{M}_{\mathbf{u},\mathbf{J}}\right)\mathbf{B}_h^n.$$

Hence our numerical approximation can be computed by

$$\begin{aligned}
\text{Solve:}\quad & D\left(\mathbb{M}_{\mathcal{V}} + \frac{\Delta t}{2}\left(\mathrm{curl}_h^T \mathbb{M}_{\mathcal{E}} + \mathbb{M}_{\mathbf{u},\mathbf{J}}\right)\mathrm{curl}_h\right) E_{h,\mathsf{Int}}^{n+1/2} = \\
& = D\left(\mathrm{curl}_h^T \mathbb{M}_{\mathcal{E}} + \mathbb{M}_{\mathbf{u},\mathbf{J}}\right)\mathbf{B}_h^n - D\left(\mathbb{M}_{\mathcal{V}} + \frac{\Delta t}{2}\left(\mathrm{curl}_h^T \mathbb{M}_{\mathcal{E}} + \mathbb{M}_{\mathbf{u},\mathbf{J}}\right)\mathrm{curl}_h\right) E_{h,\mathsf{Bound}}^{n+1/2},
\end{aligned}$$

$$\text{Plug into:}\quad E_h^{n+1/2} = E_{h,\mathsf{Int}}^{n+1/2} + E_{h,\mathsf{Bound}}^{n+1/2},$$

$$\text{Take a Step Forward:}\quad \mathbf{B}_h^{n+1} = \mathbf{B}_h^n - \Delta t \mathrm{curl}_h E_h^{n+1/2},$$

where the first step is given by the initial conditions (19c), $\mathbf{B}_h^0 = \mathscr{I}_h^{\mathcal{E}}(\mathbf{B}_0)$. It is important to note that, in order to solve the first system in our algorithm we must extract a submatrix that acts on the components of $E_{h,\mathsf{Int}}$ related to the interior nodes.

Notice that, by theorem 4.1, taking discrete divergence in equation (23a) we find that $\mathrm{div}_h \mathbf{B}_h^{n+1} = \mathrm{div}_h \mathbf{B}_h^n$ therefore if the initial conditions on $\mathbf{B}$ are divergence free then our discrete approximations will preserve this property.

6 Construction Of Mimetic Matrices

Now we turn our attention to the construction of the matrices $\mathbb{M}_{\mathcal{V}}, \mathbb{M}_{\mathcal{E}}$ and $\mathbb{M}_{\mathbf{u},\mathbf{J}}$, these are the result of an assembly of local matrices on the elements of a mesh, Ω_h, hence our focus will be on defining the local matrices from which they are assembled. In order to ease the notation we will refer to these local matrices with the same symbol as the global matrices, there is little chance for confusion since the only reference to the global matrices happens in the first sentence of this section.

Let P be an element of Ω_h which shall remain fixed. On P we will define two spaces of continuous functions, the space of reconstruction of dimension n and denoted $\mathscr{S}_h$ and one of its subspaces, with basis $\{q_1, ..., q_{\tilde{n}}\}$, refered to as the space of test functions and represented by $\mathscr{T}$.

The procedure we will describe next will define $\mathbb{M}_{\mathcal{V}}$ and $\mathbb{M}_{\mathcal{E}}$, the procedure for $\mathbb{M}_{\mathbf{u},\mathbf{J}}$ is unique and will be explained later. Let, for the sake of this discussion, $\mathscr{D}$ represent either the symbol $\mathcal{V}$ or $\mathcal{E}$ and N be a rectangular matrix whose i-th row is $\mathscr{I}_h^{\mathscr{D}}(q_i)$. Moreover define the vector R_i by the relation

$$\forall E \in \mathscr{S}_h: \quad \int_P E q_i = \mathscr{I}_h^{\mathcal{V}}(E)^T R_i,$$

in the case where $\mathscr{D} = \mathscr{V}$ and

$$\forall B \in \mathscr{S}_h: \quad \int_P \mathbf{B} \cdot q_i = \mathscr{I}_h^{\mathscr{E}}(\mathbf{B})^T R_i,$$

if $\mathscr{D} = \mathscr{E}$ and let R be a set whose i-th row is R_i. Having constructed the rectangular matrices N and R, the definition of $\mathbb{M}_{\mathscr{D}}$ follows the formula

$$\mathbb{M}_{\mathscr{D}} = R(R^T N)^{-1} R^T + \lambda(\mathrm{Id} - N(N^T N)^{-1} N^T),$$

where Id represents the identity matrix and $\lambda = \frac{2}{n}\mathrm{trace}(R(R^T N)^{-1} R^T)$, this formula is derived in chapter 4 of [2]. In the next subsections we will construct N and R for the two matrices $\mathbb{M}_{\mathscr{E}}$, $\mathbb{M}_{\mathscr{V}}$ and we finish with the construction of $\mathbb{M}_{\mathbf{u},\mathbf{J}}$. All normal vectors are picked pointing out of the element P and tangential vectors are picked in the counterclockwise direction as required by the divergence and stokes theorem and the edges on the boundary of P are $\{e_i\}_{i=1}^n$.

6.1 Local Mass Matrix in $\mathscr{E}_h$

In the case of $\mathscr{V}_h$ the spaces are

$$\mathscr{S}_h := \{\mathbf{B} : \mathrm{div}\mathbf{B} \in \mathbb{R}, \mathbf{B}|_e \cdot \hat{n} \in \mathbb{R} \text{ for all } e \in \partial P\} \qquad \text{and} \qquad \mathscr{T} := \{\nabla p : p \in \mathrm{span}\,(x - x_P, y - y_P)\},$$

where (x_p, y_p) represents the barycenter of P. By Green's formula we must have that

$$\int_P \mathbf{B} \cdot \nabla p = -\int_P \mathrm{div}\mathbf{B}\, p + \sum_{e \in \partial P} \int_e p\mathbf{B} \cdot \hat{n}^e d\ell,$$

from the fact that $\mathbf{B} \in \mathscr{S}_h$ and that, by construction, p is of zero mean when it is a member of $\mathscr{T}$ we have that

$$\int_P \mathbf{B} \cdot \nabla p = \sum_{e \in \partial P} \mathbf{B} \cdot \hat{n}^e \int_e p d\ell.$$

Thus for $e = (v_1^e, v_2^e)$, and edge of P, the fact that p is linear when restricted to e allows us to compute the line integral on the right by the midpoint rule. This is to say that

$$\int_e p d\ell = |e| p(v_{3/2}^e), \qquad v_{3/2}^e := \frac{v_1^e + v_2^e}{2}.$$

Therefore,

$$\int_P \mathbf{B} \cdot \nabla p = \sum_{e \in \partial P} \mathbf{B} \cdot \hat{n}^e p(v_{3/2}^e)|e|. \tag{24}$$

We want to find a matrix $\mathbb{M}_{\mathscr{E}}$ such that

$$[\mathbf{B}_h, W_h]_{\mathscr{E}_h} := \mathbf{B}_h^T \mathbb{M}_{\mathscr{E}} W_h \approx \int_P \mathbf{B} \cdot \mathbf{W} \qquad \mathbf{B}_h = \mathscr{I}_h^{\mathscr{E}}(\mathbf{B}),\ W_h = \mathscr{I}_h^{\mathscr{E}}(\mathbf{W}),$$

is exact whenever $\mathbf{W} \in \mathscr{T}^{\mathscr{E}}$ and $\mathbf{B} \in S_h^{\mathscr{E}}$. To ensure that this condition is satisfied it is important to note that that, by our choice of reconstruction space, the $i-$th entry of $\mathbf{B}_h$ is $\mathbf{B} \cdot \hat{n}^{e_i}$, thus the identity (24) can be interpreted as

$$\int_P \mathbf{B} \cdot \nabla p = \mathbf{B}_h^T \begin{pmatrix} p(v_{3/2}^{e^1})|e^1| \\ \vdots \\ p(v_{3/2}^{e^n})|e^n| \end{pmatrix}.$$

Thus, testing this against $\{\nabla p_1, \nabla p_2\}$ for $p_1 := x - x_P$ and $p_2 := y - y_P$, a basis for $\mathscr{T}^{\mathscr{E}}$ we arrive at arrive at

$$\int_P \mathbf{B}\cdot\nabla p_1 = \mathbf{B}_h^T R_1 \text{ and } \int_P \mathbf{B}\cdot\nabla p_2 = \mathbf{B}_h^T R_2$$

for

$$R_1 := \begin{pmatrix} \left[\frac{1}{2}\left(x_1^{e_1} + x_2^{e_2}\right) - x_P\right]|e^1| \\ \vdots \\ \left[\frac{1}{2}\left(x_1^{e_n} + x_2^{e_n}\right) - x_P\right]|e^n| \end{pmatrix} \text{ and } R_2 := \begin{pmatrix} \left[\frac{1}{2}\left(y_1^{e_1} + y_2^{e_2}\right) - y_P\right]|e^1| \\ \vdots \\ \left[\frac{1}{2}\left(y_1^{e_n} + y_2^{e_n}\right) - y_P\right]|e^n| \end{pmatrix}, \tag{25}$$

where $v_1^{e_2} := (x_1^{e_i}, y_1^{e_i})$ and $v_1^{e_2} := (x_1^{e_i}, y_1^{e_i})$. We will come back to this identity later. Let us compute the projection of $\nabla p_1 = (1,0)^T$. Pick and edge $e = (v_1^e, v_2^e)$ then

$$\hat{n}^e = \frac{1}{|e|}\begin{pmatrix} y_2^e - y_1^e \\ x_1^e - x_2^e \end{pmatrix} \quad \text{for} \quad v_1^e = \begin{pmatrix} x_1 \\ y_1 \end{pmatrix} \; v_2^e = \begin{pmatrix} x_2 \\ y_2 \end{pmatrix}.$$

Hence,

$$\frac{1}{|e|}\int_e \nabla p\cdot\hat{n}\, d\ell = \frac{y_2^e - y_1^e}{|e|},$$

Therefore, the projection of ∇p_1, denoted by N_1, is given by

$$N_1 := \begin{pmatrix} |e_1|^{-1}\left(y_2^{e_1} - y_1^{e_1}\right) \\ \vdots \\ |e_n|^{-1}\left(y_2^{e_n} - y_1^{e_n}\right), \end{pmatrix}.$$

Similarly the projection of ∇p_2, called N_2, is

$$N_2 := \begin{pmatrix} |e_1|^{-1}\left(x_1^{e_1} - x_2^{e_1}\right) \\ \vdots \\ |e_n|^{-1}\left(x_1^{e_n} - x_2^{e_n}\right) \end{pmatrix}.$$

Finally $R := [R_1, R_2]$ and $N := [N_1, N_2]$.

6.2 Local Mass Matrix in $\mathscr{V}_h$

Our reconstruction and test spaces are

$$\mathscr{S}_h := \left\{E \in H(\mathbf{curl}, \Omega) : \mathbf{curl} E \in \mathbb{R}^2\right\},$$
$$\mathscr{T}^{\mathscr{V}} := \left\{\text{curl}\mathbf{v} : \mathbf{v} = (v_x, v_y)^T, v_x \in \text{span}\left(y - y_P\right), v_y \in \text{span}\left(x - x_P\right)\right\},$$

where (x_p, y_p), again, is the barycenter of P. By integrating by parts we arrive at the following identity

$$\int_P E\,\text{curl}\mathbf{v} = \int_P \mathbf{curl} E\cdot\mathbf{v} + \sum_{e\in\partial P}\int_e \mathbf{v}\cdot E\times\hat{n}^e dS.$$

Due to the fact that $E \in S_h$ and $\mathbf{v} \in \mathscr{T}$ we know that $\mathbf{curl} E\cdot\mathbf{v}$ is of mean zero. Hence,

$$\int_P E\,\text{curl}\mathbf{v} = \sum_{e\in\partial P}\int_e \mathbf{v}\cdot E\times\hat{n}^e dS. \tag{26}$$

For $(v_1^e, v_2^e)e \in \partial P$ we have that

$$E \times \hat{n}^e = E\hat{\tau} \quad \text{for} \quad \hat{\tau} = \frac{1}{|e|}\begin{pmatrix} x_2^e - x_1^e \\ y_2^e - y_1^e \end{pmatrix} \text{ and } v_1^e = \begin{pmatrix} x_1^e \\ y_1^e \end{pmatrix},\ v_2^e = \begin{pmatrix} x_2^e \\ y_2^e \end{pmatrix}.$$

Returning to (26) we find that for $\mathbf{v} = (v_x, v_y)^T$ we have

$$\int_P E\,\mathrm{curl}\mathbf{v} = \sum_{e\in\partial P} \frac{1}{|e|}\int_e E\left(v_x(x_2^e - x_1^e) + v_y(y_2^e - y_1^e)\right) dS. \tag{27}$$

Now pick a basis for $\mathscr{T}^{\mathscr{V}}$, say $\{\mathrm{curl}\mathbf{v} : \mathbf{v} = (y_P - y, 0)^T\}$ then $\mathscr{I}_h^{\mathscr{V}}(\mathrm{curl}\mathbf{v}) = N := (1, ..., 1)$ and by (27)

$$\int_P E\,\mathrm{curl}\mathbf{v} = \sum_{e\in\partial P} \frac{1}{|e|}\int_e E(y_p - y)(x_2^e - x_1^e)d\ell. \tag{28}$$

Now parametrize the edge e as $r(t) = (v_2^e - v_1^e)t + v_1^e,\ 0 \le t \le 1$ and write the corresponding integral on the right of (28) as

$$\int_e E(y_p - y)(x_2^e - x_1^e)d\ell = |e|(x_2^2 - x_1^e)\int_0^1 \left[\left(E(v_2^e) - E(v_1^e)\right)t + E(v_1^e)\right]\left[y_P - (y_2^e - y_1^e)t - y_1^e\right]dt.$$

We use the following quadrature

$$\int_0^1 f(t)dt = \frac{1}{6}f(0) + \frac{2}{3}f(1/2) + \frac{1}{6}f(1).$$

It is important to note that this rule is exact for polynomials of second degree and, hence,

$$\begin{aligned}&\int_e E(y_p - y)(x_2^e - x_1^e)d\ell = \\ &\quad = \frac{(x_2^e - x_1^e)|e|}{6}\left[\left(E(v_1^e)(y_P - y_1)\right) + \frac{1}{4}\left(\frac{(E(v_1^e) + E(v_2^e))(2y_P - y_2^e - y_1^e)}{4}\right) + \left(E(v_2^e)(y_P - y_2)\right)\right].\end{aligned}$$

The above leads us to

$$\begin{aligned}&\int_e E(y_p - y)(x_2^e - x_1^e)d\ell = \\ &= \frac{|e|(x_2^e - x_1^e)}{6}\Big[\left((y_P - y_1^e) + (2y_P - y_1^e - y_2^e)\right)E(v_1^e) + \left((y_P - y_2^e) + (2y_P - y_1^e - y_2^e)\right)E(v_2^e)\Big] := \\ &= |e|\left(\omega_1^e E(v_1^e) + \omega_2^e E(v_2^e)\right).\end{aligned} \tag{29}$$

If $(e_0, ..., e_{n-1})$ are ordered sequentially then for $e = (v_1^e, v_2^e)$ in a counterclockwise direction then by combining (28) and (29) we find that

$$\int_P E\,\mathrm{curl}\mathbf{v} = \left(\omega_2^{e_{n-1}} + \omega_1^{e_0}\right)E(v_1^{e_0}) + \sum_{i=1}^{n-1}\left(\omega_2^{e_{i-1}} + \omega_1^{e_i}\right)E(v_1^{e_i}).$$

Finally,

$$R = \begin{pmatrix} \omega_2^{e_{n-1}} + \omega_1^{e_0} \\ \omega_2^{e_0} + \omega_1^{e_1} \\ \vdots \\ \omega_2^{e_{n-2}} + \omega_1^{e_{n-1}} \end{pmatrix}, \quad \text{where} \quad \begin{aligned} \omega_1^e &= \tfrac{1}{6}(x_2^e - x_1^e)\left[(y_P - y_1^e) + (2y_p - y_1^e - y_2^e)\right] \\ \omega_2^e &= \tfrac{1}{6}(x_2^e - x_1^e)\left[(y_P - y_2^e) + (2y_p - y_1^e - y_2^e)\right]. \end{aligned}$$

6.3 Local Matrix $\mathbb{M}_{\mathbf{u},\mathbf{J}}$

The main difficulty in the construction of $\mathbb{M}_{\mathbf{u},\mathbf{J}}$ lies in the fact that it needs to combine nodal-based functions in $\mathcal{V}_h$ and edge-based functions in $\mathcal{E}_h$. The strategy is, therefore, to estimate $(C\mathbf{J}-\mathbf{u})\times B$ at the nodes and then using $\mathbb{M}_{\mathcal{V}}$ we can find an approximation for the required bilinear form. We now focus on the construction of the necessary nodal values, note that $C\mathbf{J}-\mathbf{u}$ is a known function hence its nodal values are straight forward to compute. However, for $\mathbf{B}$ we have limited information, only its fluxes normal to the edges of P are known, this is enough information to find the projection of $\mathbf{B}$ onto some subspaces of $\left(L^2(\Omega)\right)^2$.

Consider the subspace, V, of $\left(L^2(\Omega)\right)^2$ that is spanned by the set $B := \{\mathbf{P}_1, \mathbf{P}_2, \mathbf{P}_3\}$ for

$$\mathbf{P}_1 = \begin{pmatrix}1\\0\end{pmatrix},\ \mathbf{P}_2 = \begin{pmatrix}0\\1\end{pmatrix} \text{ and } \mathbf{P}_3 = \begin{pmatrix}x\\y\end{pmatrix}.$$

We can find the projection, $\Pi\mathbf{B}$, onto V using the characterization that

$$\Pi\mathbf{B} = a\begin{pmatrix}1\\0\end{pmatrix} + b\begin{pmatrix}0\\1\end{pmatrix} + c\begin{pmatrix}x\\y\end{pmatrix} \quad \text{and} \quad \forall \mathbf{P}\in B:\ \int_P \mathbf{B}\cdot\mathbf{P} = \int_P \Pi\mathbf{B}\cdot\mathbf{P},$$

An approximation for the above integrals is posible using the inner product matrix $\mathbb{M}_{\mathcal{E}}$, yielding the system

$$\forall \mathbf{P}\in B: \quad \mathcal{I}_h^{\mathcal{E}}(\mathbf{P})^T\mathbb{M}_{\mathcal{E}}\mathbf{B}_h = a\mathcal{I}_h^{\mathcal{E}}(\mathbf{P})^T\mathbb{M}_{\mathcal{E}}\mathbf{P}_1 + b\mathcal{I}_h^{\mathcal{E}}(\mathbf{P})^T\mathbb{M}_{\mathcal{E}}\mathbf{P}_2 + c\mathcal{I}_h^{\mathcal{E}}(\mathbf{P})^T\mathbb{M}_{\mathcal{E}}\mathbf{P}_3.$$

Let N be the matrix whose columns are the interpolations of the functions in B, then this system can be written as

$$N\mathbb{M}_{\mathcal{E}}\mathbf{B}_h = N^T\mathbb{M}_{\mathcal{E}}N\vec{x},$$

where $\vec{x} = (a,b,c)^T$, and thus the constants in the expansion of $\mathbf{B}$ can be found by multiplying the degrees of freedom of $\mathbf{B}$, on the left, by $M_\Pi := (N^T\mathbb{M}_{\mathcal{E}}N)^{-1}N\mathbb{M}_{\mathcal{E}}$. Next we use the functions in B to create a matrix M_E that takes $\vec{x}$ and returns a row of function evaluations of $\Pi\mathbf{B}$ at the nodes and finally a matrix $M_{u,J}$ than takes these nodal values and returns the necessary cross product. In short

$$\mathbb{M}_{\mathbf{u},\mathbf{J}} = \mathbb{M}_{\mathcal{V}}M_{u,J}M_EM_\Pi.$$

The choice of the space V is not arbitrary, the finite element with B as its shape functions and fluxes over the edges as the edges of P is unisolvent. If P is a triangle or a square this finite element will be a low order Thomas Raviart element and proofs of unisolvency can be found in classic books on the Finite Element Method, however, for general polygons the authors of this document could not find a proof in the literature and thus a proof is provided below.

Proposition 6.1. *The finite element with domain P, shape functions B and degrees of freedom as fluxes over the edges is unisolvent.*

Proof. Let $\mathbf{B}\in V$ be such that $\mathbf{B}_h = \mathcal{I}_h^{\mathcal{E}}(\mathbf{B}) = \mathbf{0}$. In one hand by the divergence theorem implies that

$$\int_P \text{div}\mathbf{B} = 0.$$

On the other hand, since $\mathbf{B} = a\mathbf{P}_1 + b\mathbf{P}_2 + c\mathbf{P}_3$ then $\text{div}\mathbf{B} = 2c$ yielding that $c = 0$. Thus, $\mathbf{B}\in\mathbb{R}^2$ is a vector that is orthogonal to every vector normal to the edges of P, a set which contains a basis for $\mathbb{R}^2$, implying that $\mathbf{B}$ must be orthogonal to every vector on the plane from where $\mathbf{B} = \mathbf{0}$ follows as a consequence. □

7 Analysis Of The Rate Of Convergence

Let Ω represent the square $[-1,1]\times[-1,1]$, to study the degree of the method developed we will use the following test problem

$$\begin{aligned}
&\text{Find } \mathbf{B} \text{ and } E \text{ such that:} && \frac{\partial}{\partial t}\mathbf{B} = -\mathbf{curl}E \quad \text{in} \quad \Omega,\\
& && E = -\mathbf{u}\times\mathbf{B} + \nu\,\mathrm{curl}\mathbf{B} + C\mathbf{J}\times\mathbf{B} \quad \text{in} \quad \Omega,\\
&\text{subject to the initial conditions:} && \mathbf{B}(x,y,0) = \begin{pmatrix} 50e^y + x\sin(xy) - x\cos(xy) \\ 50e^x - y\sin(xy) + y\cos(xy)\end{pmatrix} \quad \text{in} \quad \Omega, \quad \text{and}\\
&\text{and boundary conditions:} && E(x,y,t) = \left[50(e^x - e^y) + \cos(xy) + \sin(xy)\right]e^t \quad \text{in} \quad \partial\Omega,
\end{aligned}$$

where $(C\mathbf{J}$ is taken to be

$$(C\mathbf{J}-\mathbf{u})(x,y) = \left(\frac{(x^2+y^2+1)(\sin(xy)+\cos(xy))}{2(50e^x - y\sin(xy)+y\cos(xy))} \qquad -\frac{(x^2+y^2+1)(\sin(xy)+\cos(xy))}{2(50e^y + x\sin(xy)-x\cos(xy))}\right)^T.$$

One can verify that the exact solution is

$$\mathbf{B}(x,y,t) = \begin{pmatrix} 50e^y + x\sin(xy) - x\cos(xy) \\ 50e^x - y\sin(xy) + y\cos(xy)\end{pmatrix}e^t \qquad E(x,y,t) = \left[50(e^x - e^y) + \cos(xy) + \sin(xy)\right]e^t.$$

To check the robustness of the method we have selected three types of meshes presented below, see Fig. 1.

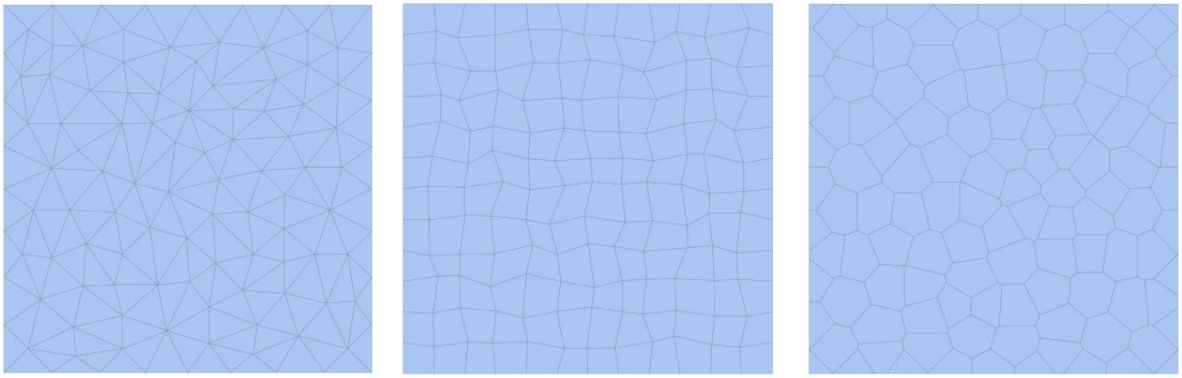

Figure 1: The the elements of the mesh on the right are triangles, in the center are perturbed squares and the rightmost is a voronoi tesselation.

The numerical results are summarized in the following tables, see Tab. 1, 2, 3.

Mesh Size	L^2 Error for Electric Field	L^2 Error for Magnetic Field
0.10101	0.25767	2.56516
0.05019	0.08600	1.43769
0.02514	0.02541	0.87187
0.01252	0.00669	0.46168
0.00626	0.00165	0.22653

Table 1: Error Analysis Results On Triangular Meshes.

Mesh Size	L^2 Error On Electric Field	L^2 Error for Magnetic Field
0.16667	0.11444	0.82392
0.08333	0.04116	0.63345
0.04347	0.01266	0.33530
0.02174	0.00328	0.16884
0.01099	0.00079	0.08424

Table 2: Error Analysis Results On Perturbed Squares.

Mesh Size	L^2 Error On Electric Field	L^2 Error for Magnetic Field
0.12803	0.48467	4.41888
0.06773	0.17629	2.49006
0.03450	0.08945	1.20755
0.01748	0.01368	0.58791
0.00878	0.006616	0.02766

Table 3: Error Analysis Results On Voronoi Tesselations.

In order to clearly see the rate of convergence of the method we plotted the errors in tables Tab. 1,2,3 in logarithmic scale in figures Fig. 2,3,4.

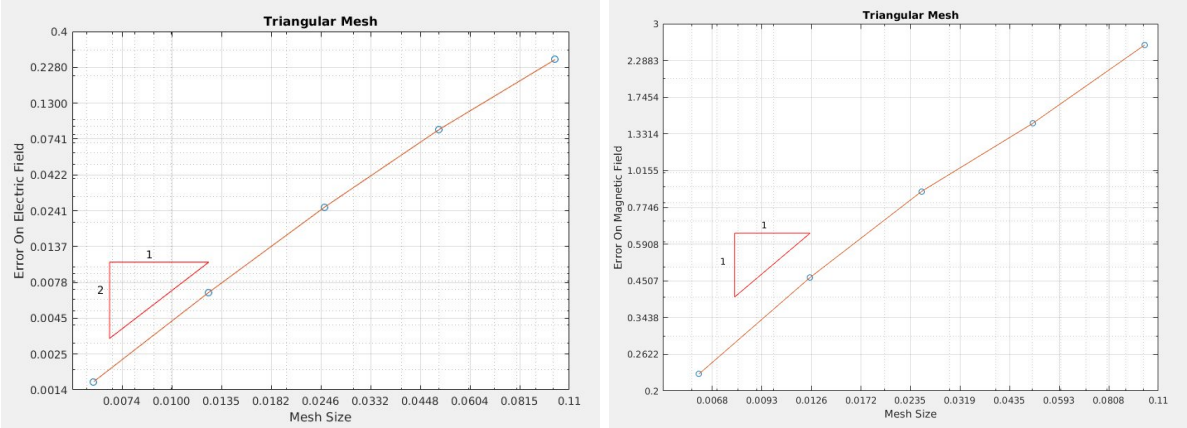

Figure 2: Error For Triangular Meshes.

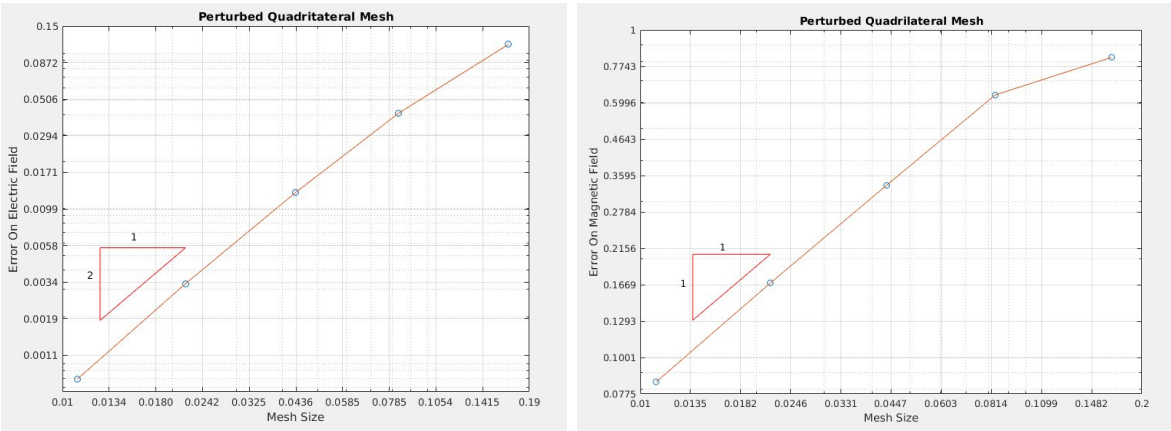

Figure 3: Errors For Perturbed Squares Meshes.

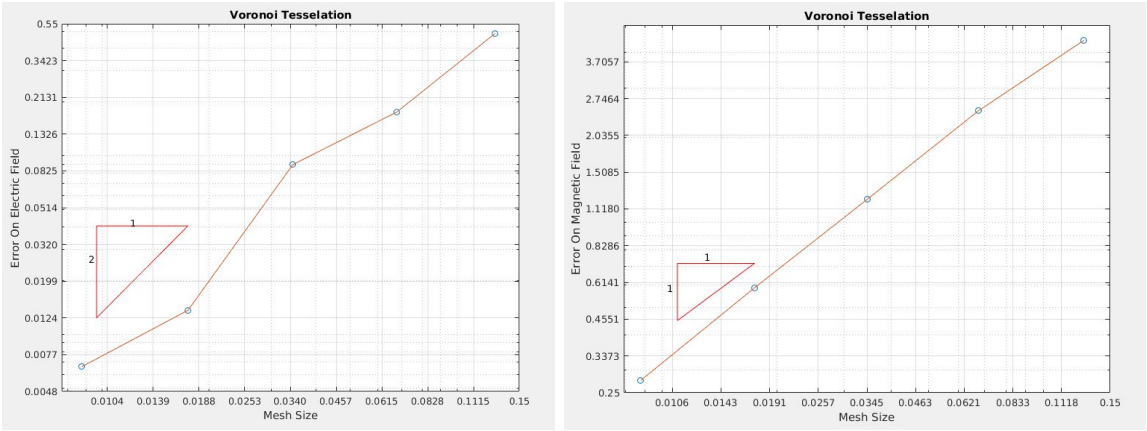

Figure 4: Errors For Voronoi Tesselations.

8 A Model For Magnetic Reconnection

In order to model the phenomenon of magnetic reconnection we used the mimetic framework presented to solve the problem where, again, Ω represents the square of side length 2 with center at the origin

$$
\begin{aligned}
&\text{Find}: \mathbf{B}, E: \\
&\frac{\partial}{\partial t}\mathbf{B} = -\mathbf{curl}E \qquad \text{in} \quad \Omega, \\
&E = -\mathbf{u}\times\mathbf{B} + \nu\text{curl}\mathbf{B} + C\mathbf{J}\times\mathbf{B} \qquad \text{in} \quad \Omega, \\
&\mathbf{B}(x,y,0) = \begin{pmatrix}\tanh y \\ 0\end{pmatrix} \qquad \text{in} \quad \Omega, \\
&E(x,y,t) = \text{const} \qquad \text{on} \quad \partial\Omega \\
&\int_{\partial\Omega}\mathbf{B}(x,y,t)\times\hat{n}d\ell = \int_{\partial\Omega}\mathbf{B}(x,y,0)\times\hat{n}d\ell.
\end{aligned}
$$

The process of magnetic reconnection can be clearly visible when plotting streamlines for the magnetic field, see Fig. 5-9.

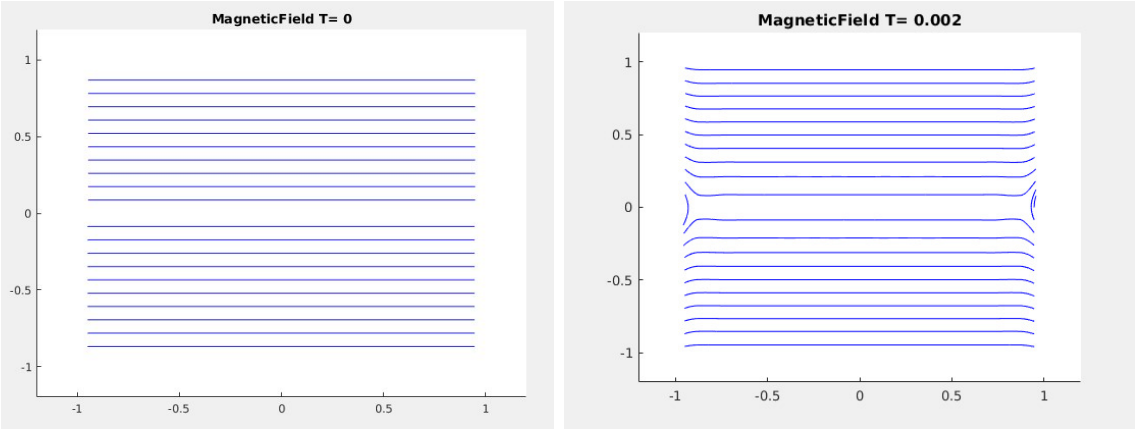

Figure 5: The left picture is that of the initial conditions, the right picture shows that reconnection happens almost inmmediately.

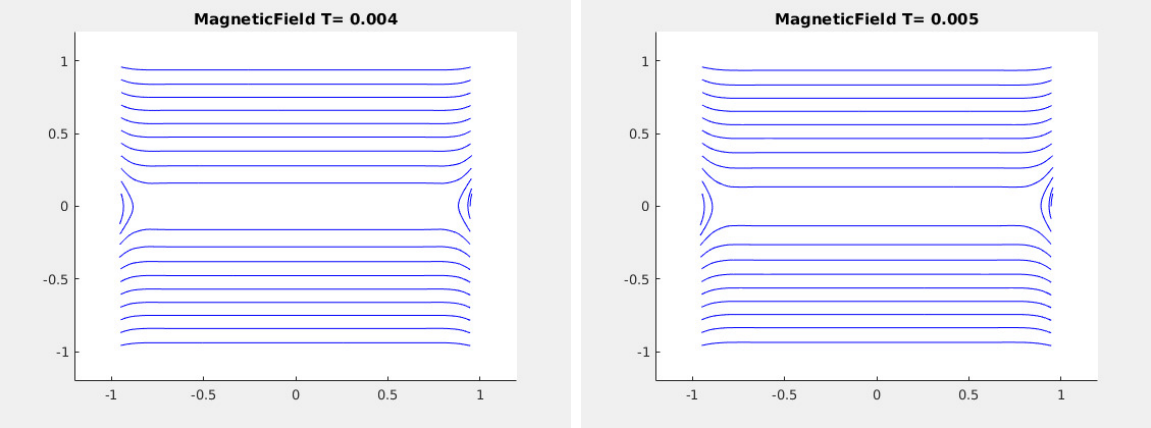

Figure 6: Withing less than a hundredth of the time unit two of the original streamlines have already reconnected.

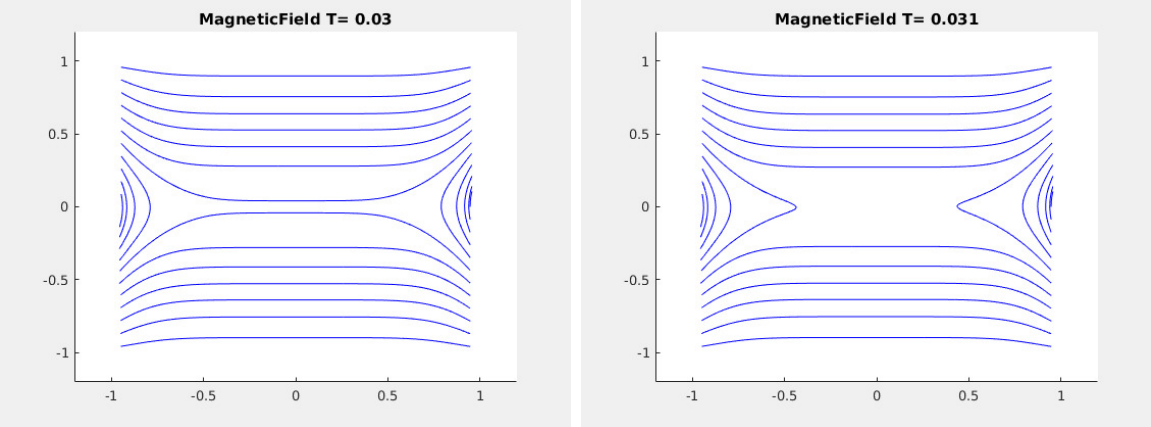

Figure 7: This pair depects exactly the moment a streamline reconnects.

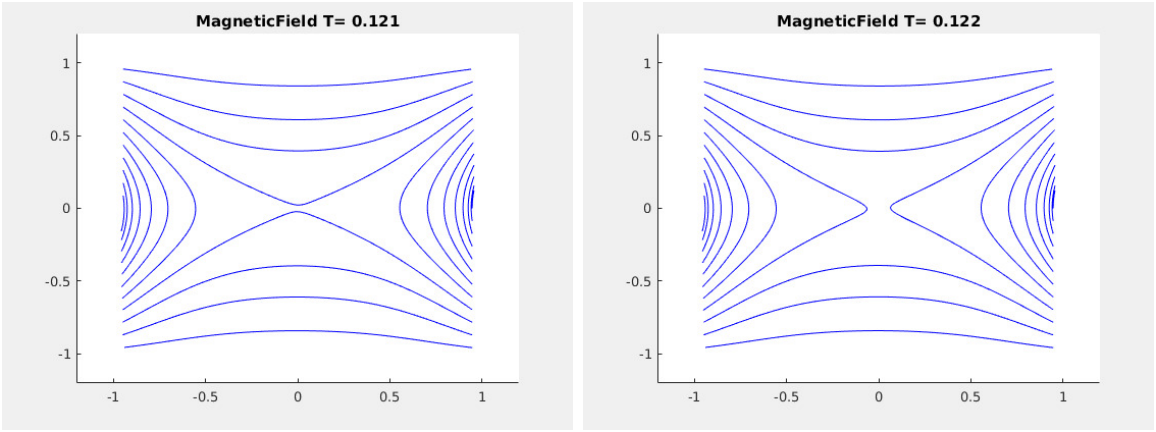

Figure 8: Reconnection happens much slower after one tenth of the time unit.

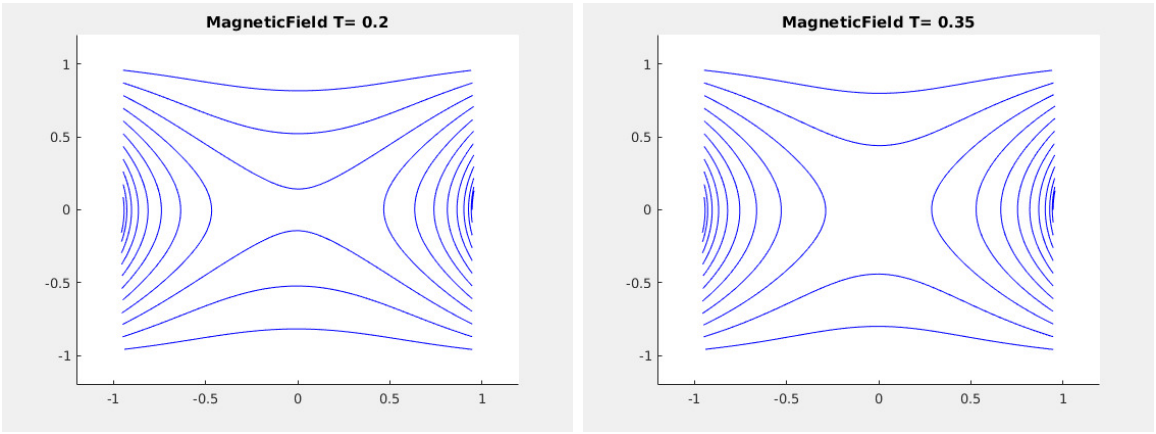

Figure 9: Finally the streamlines reach a steady state as depicted above.

9 Conclusions

We successfully constructed a MFD method for the subset of the MHD equations. Given the fact that the degrees of freedom of the electric field were placed at the nodes whereas normal fluxes accross the edges were the degrees of freedom for the magnetic field, the discretization of the term $(C\mathbf{J}-\mathbf{u})\times\mathbf{B}$ is neither standard nor straight-forward. We resolved this complication by, locally, finding an approximate projection of $\mathbf{B}$ onto a subspace of $\left(L^2(\Omega)\right)^2$, the global approximation came about after an assembly. The inner products necessary were approximated using the mimetic matrices on $\mathscr{V}_h$ and $\mathscr{E}_h$.

Numerical experiments give indication that the method constructed is convergent of degree two in the electric field and of order one in the magnetic field. However, in the case of general Voronoi tesselations the error in the electric field, although it shows a decay towards zero, does

not seem to approach a well defined slope when plotted in a logarithmic scale. Further numerical experimentation is required to explain this behavior.

The method was shown robust enough to model slow magnatic reconnection as evidenced in section 8, however fast magnetic reconnection is a non-linear phenomenon and the framework presented does not seem capable of capturing it. The reason being that the physics happen in three dimensions and not all the phenomena can be modelled in a smaller dimensional setting. This work presents a clear way to carry this project forward: develop and implement a MFD method in three dimensions, include more terms in ohms law namely:

$$E + \mathbf{u} \times \mathbf{B} = \nu \mathbf{J} + C\mathbf{J} \times \mathbf{B} + K\frac{D\mathbf{J}}{Dt},$$

where the above time derivative represents the material derivative. The final step would be to couple this system with the fluid flow equations.

10 Acknowledgements

S. Naranjo's work was carried out under the support of the National Science Foundation grants # 1545188 titled 'NRT-DESE: Risk and uncertainty quantification in marine science and policy' as well as DMS grant # 1720116.

Special thanks to Konstantine Lipnikov of the Los Alamos National Laboratory theoretical division for his advice during the writing of this report.

References

[1] Paolo Corti. Stable numerical scheme for the magnetic induction equation with hall effect. In *Hyperbolic Problems: Theory, Numerics and Applications (In 2 Volumes)*, pages 374–381. World Scientific, 2012.

[2] Lourenco Beirao da Veiga, Konstantin Lipnikov, and Gianmarco Manzini. *The mimetic finite difference method for elliptic problems*, volume 11. Springer, 2014.

[3] Peter Alan Davidson. An introduction to magnetohydrodynamics, 2002.

[4] Vitaliy Gyrya, Konstantin Lipnikov, and Gianmarco Manzini. The arbitrary order mixed mimetic finite difference method for the diffusion equation. *ESAIM: Mathematical Modelling and Numerical Analysis*, 50(3):851–877, 2016.

[5] Vitaliy Gyrya, Konstantin Lipnikov, Gianmarco Manzini, and Daniil Svyatskiy. M-adaptation in the mimetic finite difference method. *Mathematical Models and Methods in Applied Sciences*, 24(08):1621–1663, 2014.